Swiss J Geosci (2012) 105:283–297
DOI 10.1007/s00015-012-0096-2

Fluid-driven low-grade metamorphism in polydeformed rocks of Avalonia (Arisaig Group, Nova Scotia, Canada)

Isabel Abad · Fernando Nieto · Gabriel Gutiérrez-Alonso · J. Brendan Murphy · James A. Braid · Alejandro B. Rodríguez-Navarro

Received: 9 August 2011 / Accepted: 20 April 2012 / Published online: 1 August 2012

Abstract The Lower Silurian—Lower Devonian Arisaig Group (Antigonish Highlands) in the Canadian Appalachians is a sequence of shallow marine strata deposited after the accretion of Avalonia to Baltica during the closure of the Iapetus Ocean. Deformation of the strata is widely attributed to the Devonian Acadian orogeny and produced shallowly plunging regional folds and a cleavage of varying penetrativity. Phyllosilicate minerals from the finest-grained rocks exhibit very low-grade (diagenetic-anchizone) metamorphic conditions. X-ray diffraction study reveals that the sampled rocks contain quartz, K-white mica, chlorite, and feldspars; illite–smectite and chlorite–smectite mixed-layers are common but Na–K mica and kaolinite occur only in some samples. The identification of illite–smectite mixed-layers in diagenetic samples, with Kübler Index >0.50 $\Delta°2\theta$ and the highly heterogeneous *b*-cell dimension of the K-white micas are in agreement with the variable chemical composition of dioctahedral micas, which present low illitic substitution and variable phengitic content. The spatial variation in the above crystal-chemical parameters was plotted along a NW–SE composite cross section across the regional folds. No correlation was found between the metamorphic conditions and either the stratigraphic depth or the strain values measured by phyllosilicates orientation analyses, as a function of the penetrativity of the cleavage. However, the metamorphic grade generally increases towards the Hollow Fault, and is highest in samples located within a 1 km corridor from the fault surface. Incipient cleavage is observed in the anchizonal samples located in the vicinity of the Hollow Fault and in some of the diagenetic samples, indicating cleavage development under low temperatures (<200 °C). These relationships, together with regional syntheses, suggest low-grade metamorphism post-dated regional folding and was coeval with Late Carboniferous dextral movement along the Hollow Fault. Fluid circulation associated with movement along this major fault may be the driving mechanism for the increasing metamorphism towards it.

Keywords Anchizone · Appalachian orogen · Crystal-chemical parameters · Hollow Fault · Kübler Index · Orientation analysis

Editorial handling: Rafael Ferreiro Mählmann and Edwin Gnos.

I. Abad (✉)
Departamento de Geología, Universidad de Jaén,
Unidad Asociada Grupo de Geología UJA-CSIC (IACT),
23009 Jaén, Spain
e-mail: miabad@ujaen.es

F. Nieto
Departamento de Mineralogía y Petrología e IACT,
Universidad de Granada, CSIC, Av. Fuentenueva,
18002 Granada, Spain

G. Gutiérrez-Alonso
Departamento de Geología, Facultad de Ciencias,
Universidad de Salamanca, 37003 Salamanca, Spain

J. B. Murphy · J. A. Braid
Department of Earth Sciences, St. Francis Xavier University,
Antigonish, NS B2G 2W5, Canada

A. B. Rodríguez-Navarro
Departamento de Mineralogía y Petrología,
Universidad de Granada, Av. Fuentenueva,
18002 Granada, Spain

1 Introduction

The sensitivity of the crystal-chemical parameters of phyllosilicate minerals to changes in temperature, pressure

and deformation (finite strain) facilitates the characterization of the diagenetic to low-grade metamorphic evolution in sedimentary basins (Frey 1987; Merriman and Peacor 1999; Abad et al. 2010; among others). Determination of these parameters may also assess (1) the potential relationship of the diagenetic-metamorphic gradient with either the burial depth (Nieto et al. 1996) or the strain recorded in the rocks (Reinhardt 1991; Gutiérrez-Alonso and Nieto 1996; Giorgetti et al. 2000) and (2) the geodynamic environment that accompanied regional deformation and phyllosilicate mineral growth (Abad et al. 2003a).

In the Appalachian orogen of northern mainland Nova Scotia, Canada, the Arisaig Group (Antigonish Highlands) provides excellent exposures of shallow marine Lower Silurian to Lower Devonian siliciclastic sedimentary rocks that underwent low-grade metamorphism between the Early and Late Devonian (Boucot et al. 1974). The Antigonish Highlands lies within Avalonia (Fig. 1), a terrane that originated along the margin of Gondwana in the Neoproterozoic (e.g. Murphy and Nance 2002; Nance et al. 2010). Deposition of the Arisaig Group strata occurred during a particularly important time interval in the evolution of Avalonia. Regional syntheses indicate that deposition began after the accretion of Avalonia to Baltica (Murphy et al. 1996; Cocks and Torsvik 2002; Fortey and Cocks 2003; Murphy et al. 2006) during the closure of the Iapetus Ocean, whereas deformation of the strata is widely attributed to the Late Devonian Acadian orogeny (Waldron et al. 1996; Braid and Murphy 2006) which is interpreted reflect either the accretion of Avalonia to ancestral North America (Laurentia, e.g. van Staal et al. 1998, 2009) or ridge subduction during the closure of the Rheic Ocean that led to the Alleghanian-Variscan orogeny (Woodcock et al. 2007; Gutiérrez-Alonso et al. 2008).

Although the stratigraphy and structural style of the Arisaig Group has been studied in detail (Boucot et al. 1974; Braid and Murphy 2004), an understanding of its regional significance is hindered by the lack of knowledge about the P–T conditions that accompanied the growth of phyllosilicate minerals it contains. In this paper, we present a detailed characterization (crystal-chemical parameters, textural and chemical features) of the phyllosilicate minerals from the fine-grained rocks of the Arisaig Group.

Our large dataset provides new insights into the low-grade metamorphic conditions of these rocks, the clay mineral genesis, and its potential relationship to the regional deformation processes (the Early Devonian

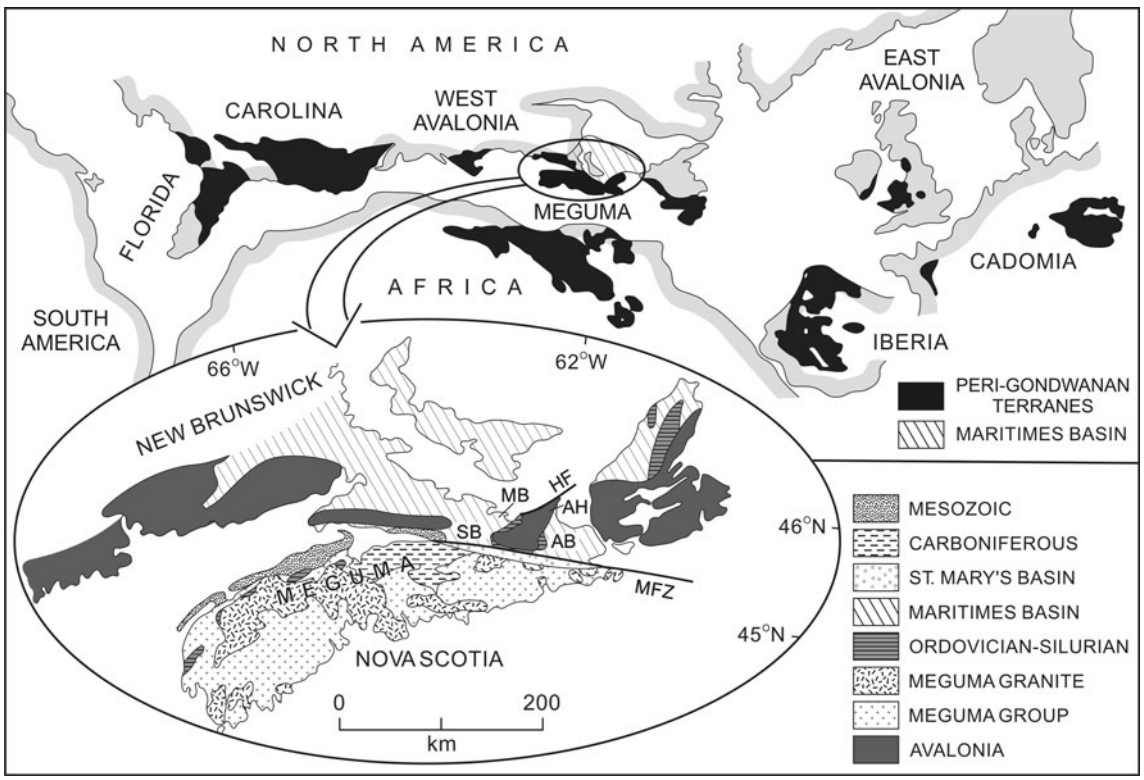

Fig. 1 Map of the North Atlantic Borderlands in their pre-Mesozoic drift positions showing the distribution of Avalonia and other Neoproterozoic peri-Gondwanan terranes (modified from Strachan and Taylor 1990; Nance and Murphy 1994). The portion of Avalonia in Atlantic Canada is identified as West Avalonia, the portion in Britain and Ireland is known as East Avalonia. Only peri-Gondwanan terranes where Cambrian overstep sequences occur are identified (see Theokritoff 1979; Keppie 1985; Murphy et al. 2004; Landing 2005). *AB* Antigonish Basin, *AH* Antigonish Highlands, *HF* Hollow Fault, *MB* Maritimes Basin, *MFZ* Minas Fault Zone, *SB* Stellarton Basin

Acadian orogeny and the Carboniferous Alleghanian orogeny). More generally, the dataset provides an example of how knowledge of crystal-chemical parameters of phyllosilicate minerals contributes to the understanding of the evolution of an orogen. We also test the correlation of the metamorphic conditions in relation to the strain values measured as a function of the penetrativity of the cleavage with phyllosilicates orientation analysis using two-dimensional diffraction patterns, obtained with a X-ray single-crystal diffractometer, which has allowed to assess the importance of other factors different from deformation in acquiring the metamorphic grade obtained in the studied rocks.

2 Geologic setting

The Arisaig Group occurs along the flanks of the Antigonish Highlands in the Avalon terrane of northern mainland Nova Scotia (Fig. 2). The group unconformably overlies (1) Upper Neoproterozoic arc-related volcanic and sedimentary rocks (Georgeville Group, Murphy et al. 1991), (2) a Cambrian-Lower Ordovician sequence of bimodal intra-continental volcanic rocks and terrestrial to shallow marine strata (e.g. Landing and Murphy 1991) and (3) a Middle to Upper Ordovician bimodal intra-continental volcanic rocks and interbedded red clastic sediments, known as the Dunn Point and McGillivray Brook formations north of the Hollow Fault and the coeval Bears Brook Formation south of the Hollow Fault (Fig. 2; Hamilton and Murphy 2004). The Arisaig Group was deformed into NE-trending regional folds in the Middle Devonian and is unconformably overlain by Middle to Upper Devonian basalts and continental redbeds of the McArras Brook Formation.

2.1 Stratigraphy

The Arisaig Group is described in detail by Boucot et al. (1974), Murphy (1987), Waldron et al. (1996) and Meyer et al. (2008). It consists of 1,800–1,900 m continuous stratigraphic sequence that is Llandoverian to Lochkovian in age and is dominated by unmetamorphosed shallow marine fossiliferous siliciclastic rocks (Fig. 3a). The basal Lower Llandovery Beechill Cove Formation contains

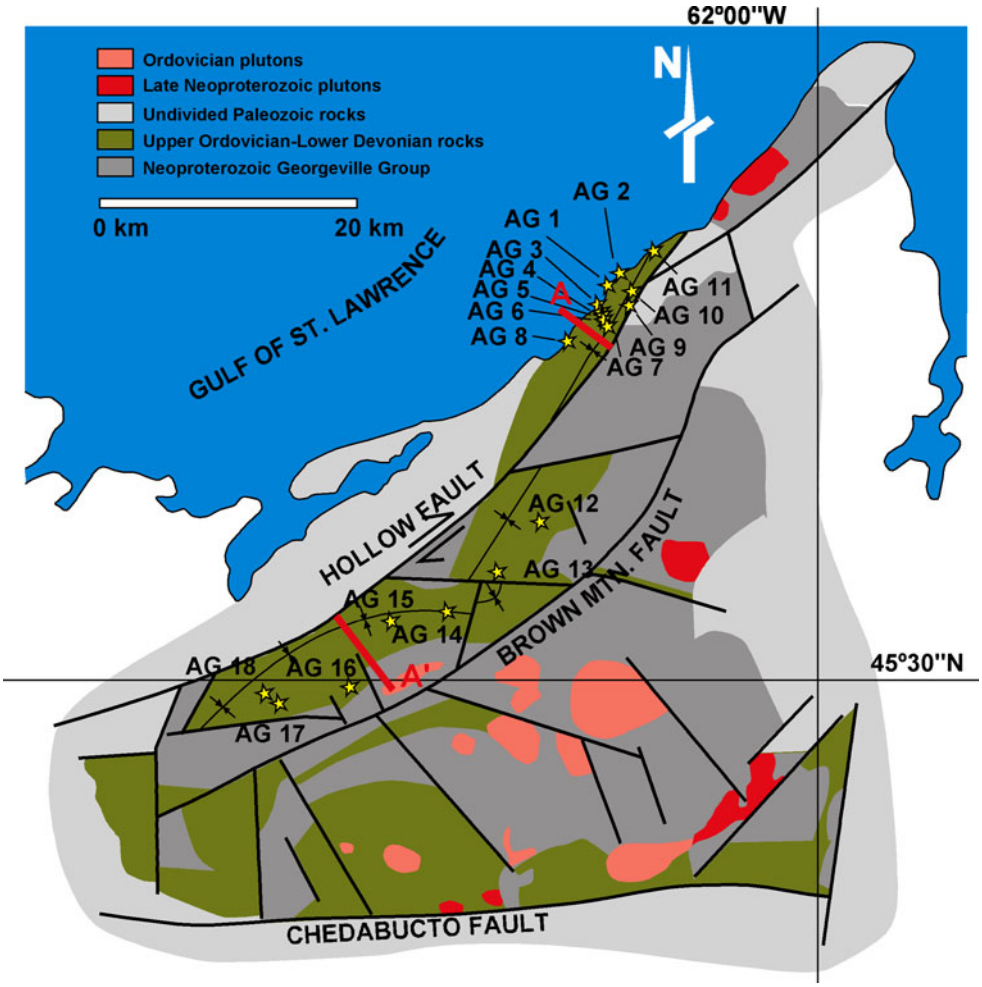

Fig. 2 Simplified geological map (after Murphy et al. 1991, modified by Escaragga et al. 2012) with the cross section sampled along Arisaig Group as A–A′. The sampling locations are represented by *stars*

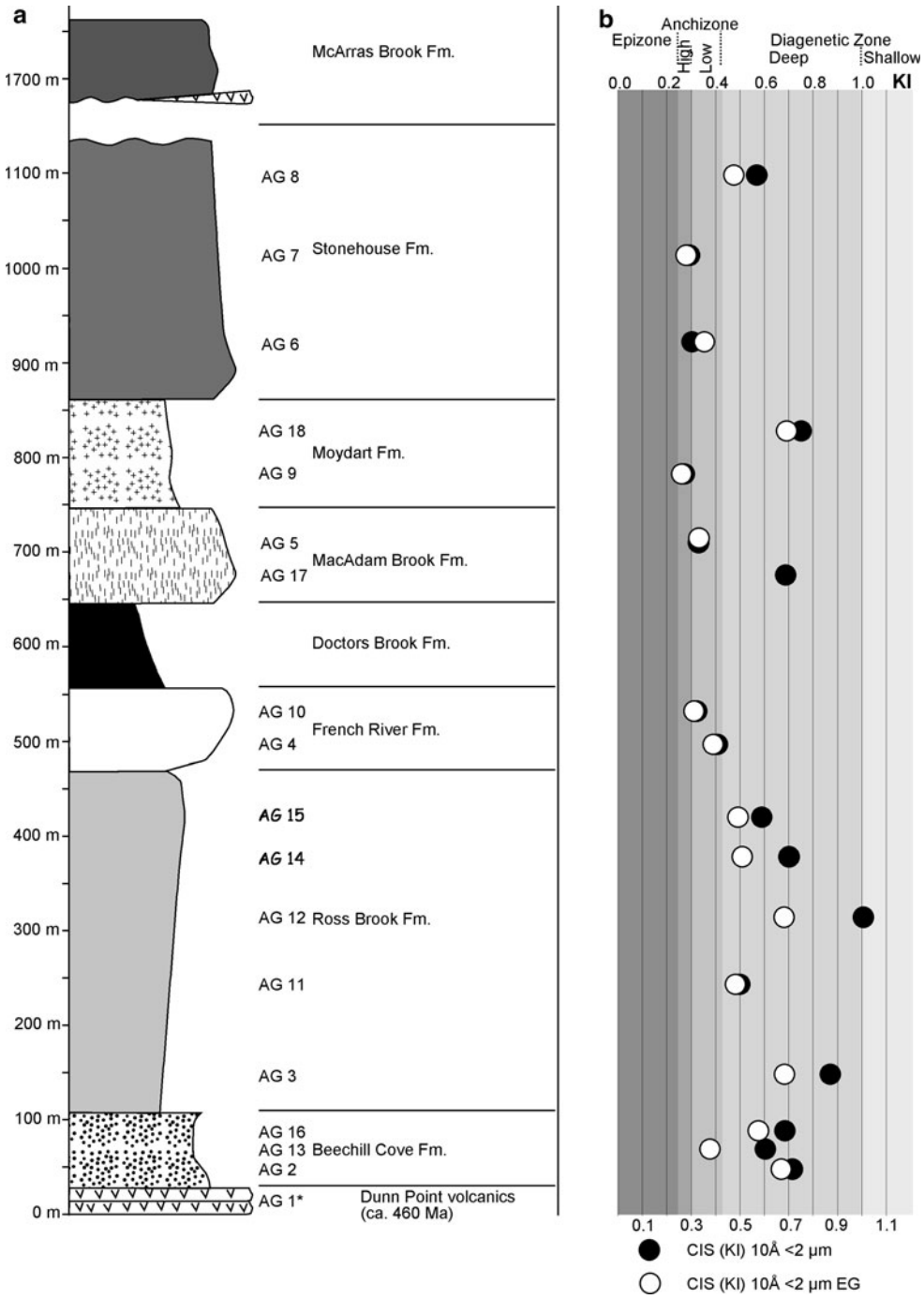

Fig. 3 **a** Stratigraphic column of the Arisaig Group rocks showing the position of the samples and **b** Kübler Index (KI) values. The Knoydart Formation, above the Stonehouse Formation and ca. 340 m thick has not been represented due to the absence of samples collected from this formation

conglomerate and shale deposited in a near shore environment, overlain by interbedded mudstone, shale and sandstone (Pickerill and Hurst 1983). The Middle to Upper Llandovery Ross Brook Formation consists of graptolite-bearing black shale, muddy siltstone, arenaceous limestone and ash (K-bentonite) beds (Boucot et al. 1974; Hurst and Pickerill 1986; Bergström et al. 1997), and is conformably overlain by the Wenlockian French River Formation, a sequence of interbedded green fissile shale, siltstone, and sandstone and minor ironstone. The overlying Upper Wenlockian Doctors Brook Formation consists of interbedded laminated shale, minor siltstone, and arenaceous limestone and is conformably overlain in turn by interbedded fissile shale, calcareous siltstone, and fossiliferous limestone, minor ash beds of the Lower Ludlovian MacAdam Brook Formation and by green interbedded siltstone, shale, mudstone, and subaerial red mudstone of the Upper Lludlovian Moydart Formation (Dineley 1963; Lane and Jensen 1975). These strata are conformably overlain by interbedded mudstone, shale with minor siltstone and

sandstone of the Pridolian Stonehouse Formation, followed by subaerial interbedded red and green coarse to fine-grained clastic rocks of the Knoydart Formation (Boucot et al. 1974).

According to Waldron et al. (1996), Arisaig Group basin development began with an Early Llandovery phase of rapid subsidence and extension (30–60 %), followed by thermal relaxation and slower subsidence rates in the Wenlockian and Ludlow. In the Pridoli, deposition of the Stonehouse Formation was coeval with vastly increased subsidence rates and accommodation space.

2.2 Structure

The strata were deformed into regional NNE-trending folds prior to the deposition of the Middle to Upper Devonian McArras Brook Formation, which is only moderately tilted (typically dips of 40° or less) and displays no internal

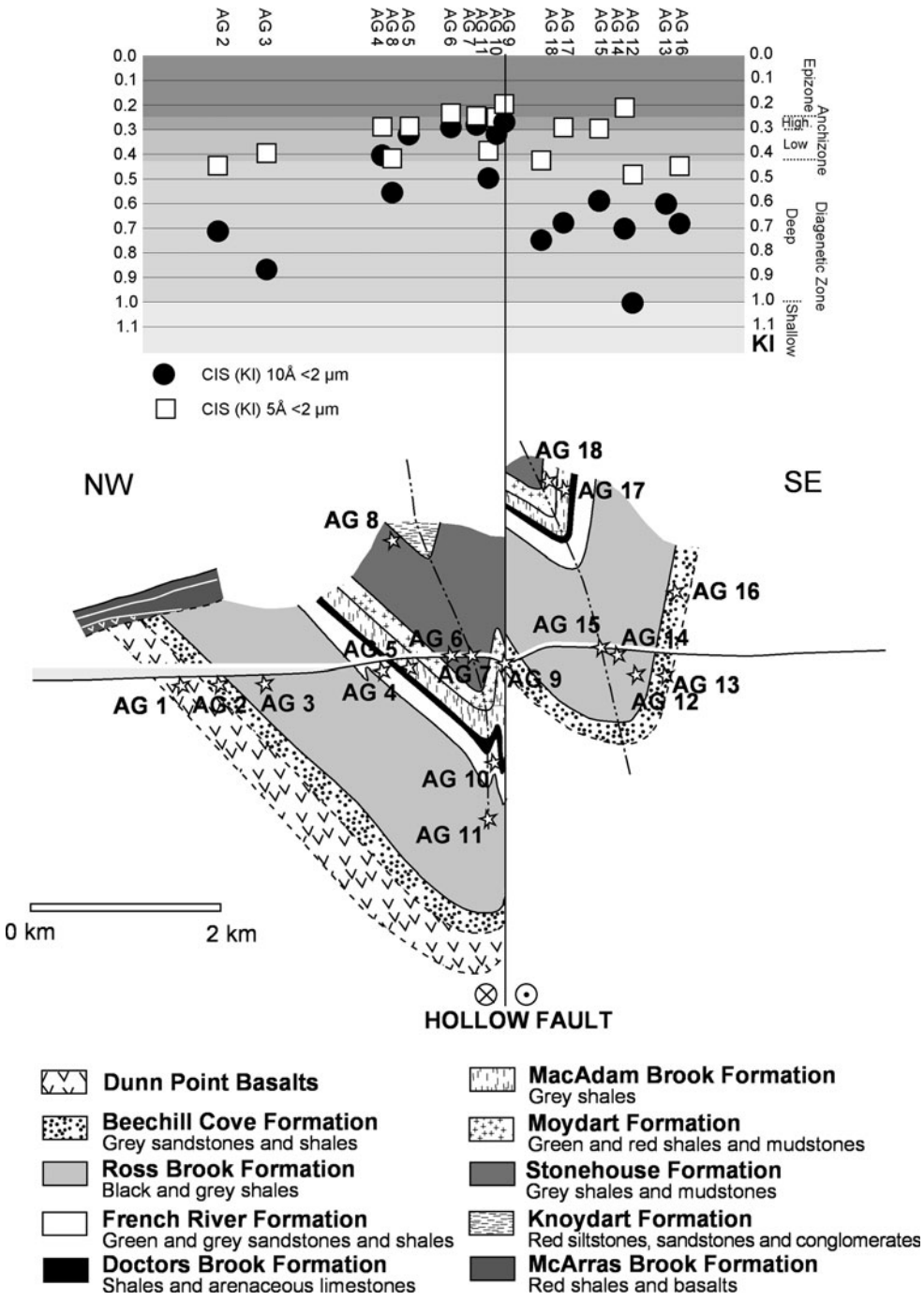

Fig. 4 Composite cross section across shallow plunging synclinal affected by the Hollow Fault showing the Kübler Index (KI) values of the studied samples

deformation (Boucot et al. 1974; Braid and Murphy 2006). These relationships suggest an Early to Middle Devonian age of deformation.

North of the Hollow Fault, the Arisaig Group strata are folded into a large-scale (km scale wavelength) NNE-NE D_1 asymmetric syncline with subsidiary minor folds (Figs. 2, 4) that plunge gently to the SW. An axial planar cleavage is penetrative in shale but is non-penetrative in siltstone and sandstone. Cleavage-bedding intersection lineations (L_1) plunge gently to the southwest and are subparallel or slightly shallower than the regional fold axis. Sedimentary structures provide way-up criteria indicating that the steep north-western limb of the syncline is generally steeply dipping and commonly overturned. Boucot et al. (1974) noted a gradual opening of the fold with a slight increase in plunge and an increase in fold symmetry across the hinge.

To the south of the Hollow Fault, the Arisaig Group strata adjacent to the fault (i.e. <3 km) display similar structures and are also folded into a km-scale syncline (Fig. 4; Benson 1974; Murphy et al. 1991). However, Neoproterozoic (Georgeville Group) strata, which unconformably underlie Arisaig Group rocks along the southern flank of the syncline, do not exhibit these structures, suggesting that folding predominantly occurred within a few km of the Hollow Fault.

2.3 Role of the Hollow Fault

The Hollow Fault is one of the most important lineaments in the Canadian Appalachians and preserves evidence for repeated episodes of movement in a variety of tectonic settings between the Late Neoproterozoic and Late Paleozoic (Murphy et al. 1999). The close proximity of the folds in Arisaig Group strata to the NE-trending Hollow Fault and their absence in correlative strata in southern and eastern Antigonish Highlands suggest a genetic relationship between folds and movement along the Hollow Fault. Early to Middle Devonian transpressive and dextral motion along the Hollow Fault is characterized as a local response to the regionally widespread Acadian Orogeny (Braid and Murphy 2006).

Several studies indicate that the Hollow Fault also had significant dextral movement during the Late Carboniferous Alleghanian orogeny. This movement resulted in the offset of previous Acadian folds as well as local zones of either basin development (Yeo and Ruixiang 1987; Waldron 2004) or zones with pervasive deformation (Murphy et al. 1999, 2011) in areas immediately adjacent to the Antigonish Highlands.

Although the effects of the Alleghanian orogeny on Arisaig Group strata have not been documented, regional studies indicate that the Hollow Fault was re-activated during the Carboniferous producing the Stellarton Basin (Waldron 2004) with faults and polydeformation characterized by reverse faults and local isoclinal folding (Murphy et al. 2011).

3 Methods

3.1 Sampling strategy

Seventeen samples were collected along the composite cross section in order to record any variations in metamorphic grade across the whole range using the illite crystallinity technique (Kübler 1968) and to establish the metamorphic conditions. Six shale samples were selected as representative of the various degrees of foliation development (deformation features) observed in the rocks at outcrop scale to be studied in detail through a X-ray single-crystal diffractometer used as a X-ray texture diffractometer in order to characterize the variations in the foliation. In particular, field observations indicate clear differences regarding the development of a penetrative foliation. Three samples were studied in more detail by scanning electron microscopy (SEM) to get a better understanding on the nature and origin of the development of the metamorphic phyllosilicates in relation with the deformation in the rocks.

Samples were collected in the Beechill Cove (3), Ross Brook (5), French River (2), MacAdam Brook (2), Moydart (2), and Stonehouse (3) formations and are representative of the whole stratigraphy of the region (Fig. 4). In order to assess their relationship with Acadian deformation, the samples have been plotted along a composite section across the shallowly plunging "Acadian" folds that crop out in the northern Antigonish Highlands. These folds have variable axial planar cleavage development (locally penetrative, generally non-penetrative), and have been attributed to transpressional deformation coeval with the movement of a major NE-trending dextral strike-slip fault (Hollow Fault, Murphy and Keppie 1998; Braid and Murphy 2006).

3.2 X-ray diffraction

The seventeen studied samples were washed and, after coarse crushing, homogeneous rock chips were used for preparation of X-ray diffraction (XRD) samples to determine the overall trends in mineral assemblages and record any variations in metamorphic grade along the studied cross sections using the Kübler Index (Kübler 1968). Currently, the Kübler Index is the most common method used to determine the metamorphic grade and to identify variations in the anchizone conditions between diagenesis and low-grade metamorphism in metapelitic sequences.

This index is based in the measurement of the full peak width at half maximum intensity of the first, 10 Å, X-ray powder-diffraction peak of K-white mica and it is expressed as $\Delta^{\circ}2\theta$ in the Bragg angle.

Whole-rock samples and clay fractions (<2 μm) were studied using a Philips PW 1710 powder diffractometer with Cu$K\alpha$ radiation, graphite monochromator and automatic divergence slit at the Departamento de Mineralogía y Petrología of the Universidad de Granada. The <2-μm fractions were separated by repeated extraction of supernatant liquid subsequent to settling. Oriented aggregates were prepared by sedimentation on glass slides. Ethylene glycol (EG) and dimethyl sulfoxide (DM) treatments were carried out on selected samples to corroborate the identification of illite–smectite, chlorite–smectite, and kaolinite on the basis of the expansibility of these phases. Preparation of samples and experimental conditions for illite "crystallinity" (Kübler Index, KI) measurements were carried out according to IGCP 294 IC Working Group recommendations (Kisch 1991). Our KI measurements (x) were transformed into crystallinity index standard (C.I.S.) values (y) according to the equation $y = 1.918x - 0.0723$ ($r = 0.999$), obtained in the laboratory using the international standards of Warr and Rice (1994). KI values were measured for the <2-μm air-dried fractions, <2-μm EG-treated fractions, and for the bulk-rock samples. In addition to the 10 Å peak, the 5 Å reflection was also measured to check the effect of other mineral phases on the former measurement following the procedures of Nieto and Sanchez-Navas (1994) and Battaglia et al. (2004). The b-cell parameters of micas and chlorites were obtained from the (060) peaks measured on slices of rock cut normal to the main foliation of the samples (Sassi and Scolari 1974). Such slices are essentially perpendicular to the (001) planes of phyllosilicates and thus avoid interference from peaks other than (060) (Frey 1987). The basal spacing of micas (d_{001}), which are related with their chemical composition (Guidotti et al. 1992), were also determined. For all spacing measurements, quartz from the sample itself was used as internal standard.

Following the XRD and optical study, six samples were prepared for the characterization of the fabrics. Samples were cut in 1 × 1 cm in slices and were analysed using a X-ray single-crystal diffractometer equipped with a CCD area detector (D8 SMART APEX, Bruker, Germany). For the diffraction experiments, the working conditions were: Mo$K\alpha$ ($\lambda = 0.7093$ Å), 50 kV and 30 mA, a pin-hole collimator of 0.5 mm in diameter, and an exposure time of 20 s per frame. Diffractometer angles ω and 2θ were set at 10 and 20°, respectively, to analyze the samples in reflection mode. A set of 2D diffraction patterns was obtained while rotating the sample around Φ angle (a frame every 5°). To determine the scattering or the degree of preferential orientation of clay basal planes, all frames were added and the intensity profile along the 00l Debye–Scherrer rings associated with these planes was calculated. The preferential orientation of the crystals with their basal planes parallel to the foliation concentrates the intensity in arcs as these planes reflect on the same portion of the ring. Thus, the width of the broad bands (angular spread, AS) displayed along the intensity profile of these rings is a gauge of the scattering in the orientation of 00l planes (Fig. 5). Additionally, pole figures for main chlorite and mica (001) reflections were calculated from the registered frames using XRD2Dscan software (Rodríguez-Navarro 2006). These pole figures represent the intensity variation of (001) reflections as a function of the sample orientation.

3.3 Scanning electron microscopy

Three samples were selected to cover different metamorphic grades and various degrees of foliation development for electron microscopy study on the basis of the crystal-chemical parameters, the mineral assemblages and field observations. Carbon-coated polished thin sections were examined by SEM, using back-scattered electron (BSE) imaging and energy-dispersive X-ray (EDX) analysis to obtain textural and chemical data. These observations were carried out using a Zeiss DSM 950 SEM, equipped with an X-ray Link Analytical QX-20 EDX system and a Leo

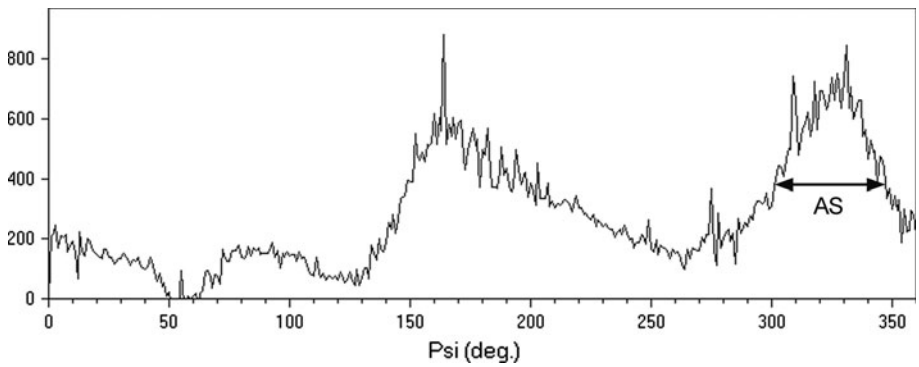

Fig. 5 Chlorite intensity profile along its (002) Debye–Scherrer ring, displaying a band with a value of angular spread (AS) equal to 46.7° (sample AG-3), that is, a moderate degree of orientation of its basal planes

1430-VPSEM at the Centro de Instrumentación Científica (C.I.C.) of the Universidad de Granada. An accelerating voltage of 20 kV, with a beam current of 1–2 nA and counting time of 50 s were used to analyse the silicates by SEM, using the following standards: albite (Na), periclase (Mg), wollastonite (Si and Ca), and orthoclase (K), and synthetic Al_2O_3 (Al), Fe_2O_3 (Fe) and $MnTiO_3$ (Ti and Mn). When such conditions, equivalent to the routine microprobe analyses, are used, major element data reach an accuracy level similar to the latter technique (see Table 2 in Abad et al. 2003b).

The structural formulae of micas were calculated on the basis of 22 negative charges $O_{10}(OH)_2$. Following Guidotti et al. (1994), we assumed that 75 % of the Fe in the micas is Fe^{3+}. The chlorite formulae were calculated on the basis of 28 negative charges.

4 Results

4.1 Mineralogy and crystal-chemical parameters

The XRD results are depicted in Table 1. With the exceptions of fine-grained sandstone AG-13 and siltstone AG-17, the rest of the samples are shales showing very homogeneous whole-rock composition. The sampled rocks contain ubiquitous quartz, K-white mica, chlorite, and feldspar; illite–smectite (I/S) and chlorite–smectite (C/S) mixed-layers are common in the clay fraction, but Na–K mica and kaolinite occur only in some samples.

Kübler Index (KI) values measured in the 10 Å peak of the <2 μm fraction are indicative of a range from diagenesis to high anchizone (Kübler 1968). The metamorphic grade varies and, in general, increases in samples closest to the Hollow Fault (especially in those ones located within 1 km from the fault surface, Figs. 2 and 4). In samples for which the widths of the 10 and 5 Å peaks are very similar, K-white mica is the only 10 Å mineral phase present. In samples where the 10 Å peaks are wider than the 5 Å peaks, other mineral phases (I/S, C/S and Na–K mica) are thought to interfere with the 10 Å peak (Nieto and Sanchez-Navas 1994; Battaglia et al. 2004). These latter samples present KI measured on <2 μm EG-treated fractions clearly lower than those of the <2 μm air-dried fractions, which demonstrates the presence of I/S mixed-layers (Nieto and Sanchez-Navas 1994). In fact, the presence of I/S mixed-layers in samples with KI >0.50° 2θ indicates diagenetic conditions (Table 1; Fig. 4). The lack of homogenization of the chemical composition of the K-white micas, indicated by highly heterogeneous b-cell dimension (average value 9.013 Å; SD 0.017Å) and basal spacing of micas (d_{001}, values between 9.957–10.009 Å) are also typical of diagenetic conditions.

In most of the samples, the peak at 14 Å (corresponding to chlorite) is small, and is absent after EG and DM treatments, reflecting high Fe contents (Brown 1961) and low quantities of chlorite.

4.2 Phyllosilicate orientation analysis of the rock fabrics by two-dimensional diffraction patterns

The preferential orientation of the crystals with their basal planes parallel to the foliation of the slate concentrates the intensity of 00l reflections in arcs as these planes reflect on the same portion of their associated Debye–Scherrer ring. Thus, the width of bands displayed in the intensity profile of these rings is a measure of the angular spread (AS) in the orientation of basal planes (Fig. 5). The smaller the AS value, the strongest is the preferential orientation of crystals and the smaller the scattering in the orientation of these planes. The AS values for chlorite and muscovite obtained for the analyzed samples under the X-ray single-crystal diffractometer are given in Table 2 and reflect the preferential orientation of the phyllosilicate grains. The smaller AS values in samples AG-3, AG-7, and AG-8 than in samples AG-2, AG-12, and AG-15 are interpreted to represent a higher amount of phyllosilicate crystals oriented in the same plane which is related to the existence of a more penetrative tectonic fabric. The pole figures graphically illustrate these results (Fig. 6), which are in coherence with field observations. Samples in the center of the cross section, closer to the Hollow Fault (Fig. 4) show a stronger preferred orientation of the phyllosilicates, which is interpreted as due to the presence of a more penetrative cleavage as can be also in concordance with the cleavage penetrativity observed in thin section.

Nevertheless, when the AS values are compared to the KI data of each sample, there seems to be no relationship between the degree of preferential orientation of clay basal planes parallel to the foliation of the slates and the illite "crystallinity". Figure 7 shows that the lowest AS values (samples with the highest preferential orientation of phyllosilicates) are found indifferently in diagenetic or anchizonal samples, and are also independent of the sample distance from the Hollow Fault. Although the samples with a higher phyllosilicate preferred orientation coincide with samples close to the fold axial plane, the change in metamorphic grade corresponds to distance from the Hollow Fault.

4.3 SEM observations

4.3.1 Texture

Backscattered scanning electron (BSE) images of selected samples show that these are quartz-rich rocks of fine-grained texture with phyllosilicate microdomains (predominantly

Table 1 UTM coordinates, lithology, crystal-chemical parameters and bulk mineralogy of very low-grade metamorphic rocks of Arisaig Group

	Coordinates (UTM-N20)		Lithology	CIS (KI)				*b* Ms (Å)	d_{001} (Å) bulk		*b* Chl (Å)	Fe Chl	Mineral composition Chl, K-rich mica, Qz (all the samples)
				10 Å		5 Å	10 Å						
	Easting	Northing		<2 μm	<2 μm EG	<2 μm	Bulk		Ms	Chl			
AG-2	E565287	N5068529	Shale	0.73	0.68	0.43	0.57		9.980	14.136			Ab, Kln, I/S
AG-3	E564341	N5067451	Shale	0.87	0.68	0.40	0.54			14.114	9.308	2.9	I/S
AG-4	E564869	N5066666	Shale	0.39	0.41	0.28				14.109			Ab, C/S
AG-5	E564827	N5066306	Shale	0.33	0.33	0.30	0.19	8.997		14.164	9.291	2.4	Ab, C/S
AG-6	E564967	N5066044	Shale	0.32	0.36	0.25	0.21	9.039	9.961	14.153	9.301	2.7	Ab, C/S
AG-7	E565040	N5065853	Shale	0.29	0.28	0.27	0.25		9.957	14.170			Ab
AG-8	E361653	N5065422	Shale	0.56	0.46	0.42	0.39	9.018	9.969	14.225			I/S, Kln
AG-9	E567244	N5067623	Shale	0.28	0.27	0.20	0.15	9.005	9.976	14.147	9.289	2.3	Ab, C/S, Or
AG-10	E567582	N5068430	Shale	0.33	0.32	0.26	0.20		10.009	14.131	9.312	3.1	Ab, Cc, C/S, Or, Na–K mica
AG-11	E568618	N5069982	Shale	0.50	0.47	0.38	0.13		10.003	14.120	9.309	3.0	I/S, Ab, Or, C/S
AG-12	E556102	N5051743	Shale	1.02	0.69	0.47			9.969	14.092			Fsp, I/S
AG-13	E554619	N5049186	Sandstone	0.61	0.37		0.26		9.961	14.136			Ab, I/S, C/S
AG-14	E554222	N5048485	Shale	0.70	0.51	0.21	0.30	8.995	9.978	14.142			I/S, Fsp, C/S, Kln
AG-15	E550113	N5047420	Shale	0.59	0.49	0.30	0.45		9.961	14.114			Fsp, I/S, C/S
AG-16	E544970	N5045355	Shale	0.68	0.58	0.43	0.28		9.976	14.142			Ab, I/S, C/S
AG-17	E541307	N5043643	Siltsone	0.68		0.32	0.43	9.026	9.971	14.131			Ab, I/S, C/S
AG-18	E540146	N5043478	Shale	0.75	0.69	0.42	0.30		9.957	14.164			Ab, I/S, C/S

Mineral abbreviations according to Whitney and Evans (2010): *Ab* albite, *Chl* chlorite, *Fsp* feldspar, *Kln* kaolinite, *Or* orthoclase, *Qz* quartz, *I/S* illite-smectite mixed-layers, *C/S* chlorite-smectite mixed-layers

Table 2 Width of the broad bands measured at half maximum intensity (AS) displayed along the Chl (002) and Ms (002) intensity profiles

	AS Chl	AS Ms
AG-2	>120	>120
AG-3	47	56
AG-7	56	73
AG-8	54	58
AG-12	73	56
AG-15	81	83

Mineral abbreviations according to Whitney and Evans (2010): *Chl* chlorite, *Ms* muscovite

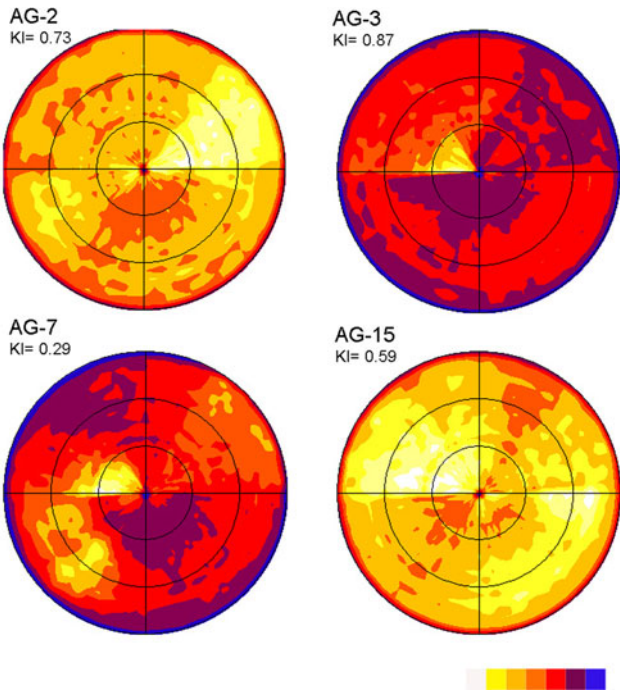

Fig. 6 Pole figures showing the orientation of (002) planes of chlorite crystals in the analyzed samples. The *colour* is related with diffraction intensity and represents the amount of crystals oriented in the same direction. The maximum colour intensity corresponds to the strongest preferential orientation of the crystals

white mica and chlorite) and iron sulphides and titanium oxides as common accessory minerals. The diagenetic sample AG-2 preserves no evidence of fabrics that could be attributed to a tectonic origin (Fig. 8a). In spite of its diagenetic grade (Fig. 4), sample AG-3 displays clear textural differences from AG-2, showing incipient development of a foliation (Fig. 8b), in agreement with the AS values (Table 2) and pole figures (Fig. 6). Sample AG-10, from near the fault plane, is characterized by incipient slaty cleavage defined by sub-parallel packets of phyllosilicate minerals, which in places form chlorite-mica stacks with curved shapes (Fig. 8c).

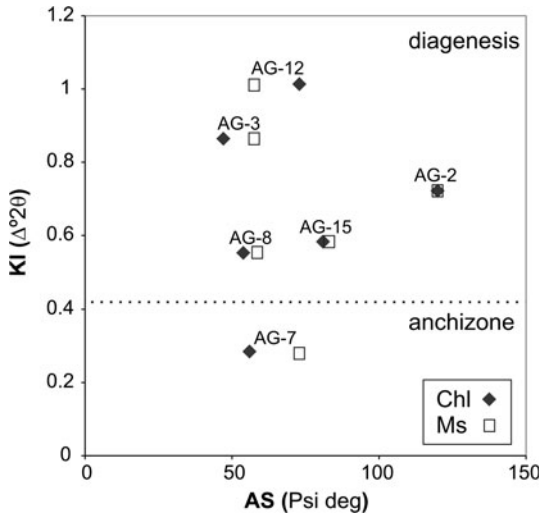

Fig. 7 Plot showing the relation between the Kübler Index (KI) values and the angular spread (AS), as an indication of the orientation degree, for the (002) reflection of chlorites (Chl) and muscovites (Ms) for the analyzed samples by a X-ray single-crystal diffractometer

4.3.2 *Chemical composition of silicates*

The chemical compositions of dioctahedral micas are presented in Table 3. They are quite variable within each sample, with an almost complete absence of illitic substitution (Σinterlayer >0.8 atoms per formula unit (a.p.f.u.) and lack of correlation between the interlayer population and Si content, $r = -0.27$) and variable phengitic content (Fe + Mg = 0.1–0.5 a.p.f.u., average value of Si = 3.16 a.p.f.u.). Such characteristics point to a possible detrital origin of analysed micas due to their greater size than the <2 μm fraction analysed by XRD. Na is generally present in low quantities (<0.15 a.p.f.u.) in most of the white micas analysed and Ca (also analysed) has not been included in the table as it is present in proportions ≤0.01 a.p.f.u. Although Ti is not abundant in white micas, it has been measured in almost all the analyses; its presence is probably linked to minor titanium oxide intergrowths within the K-rich dioctahedral micas.

Trioctahedral chlorites (Table 4) correspond to the chamosite variety with a high Fe/(Fe + Mg) ratio (0.56–0.85). The sum of octahedral cations is almost always <6 a.p.f.u. and a slight contamination by interlayer cations (K and Na) has been detected in almost all the chlorite analyses. These data are, in part, the result of the unavoidable overlapping of the beam on material other than the mineral under investigation due to the very fine-grained nature of the samples.

Kaolinite, analyzed in sample AG-2 (Fig. 8a), has an Al-rich composition, with very minor quantities of Fe, Mg, and alkaline elements probably due to the contamination with other phases, such as white mica. Analyzed

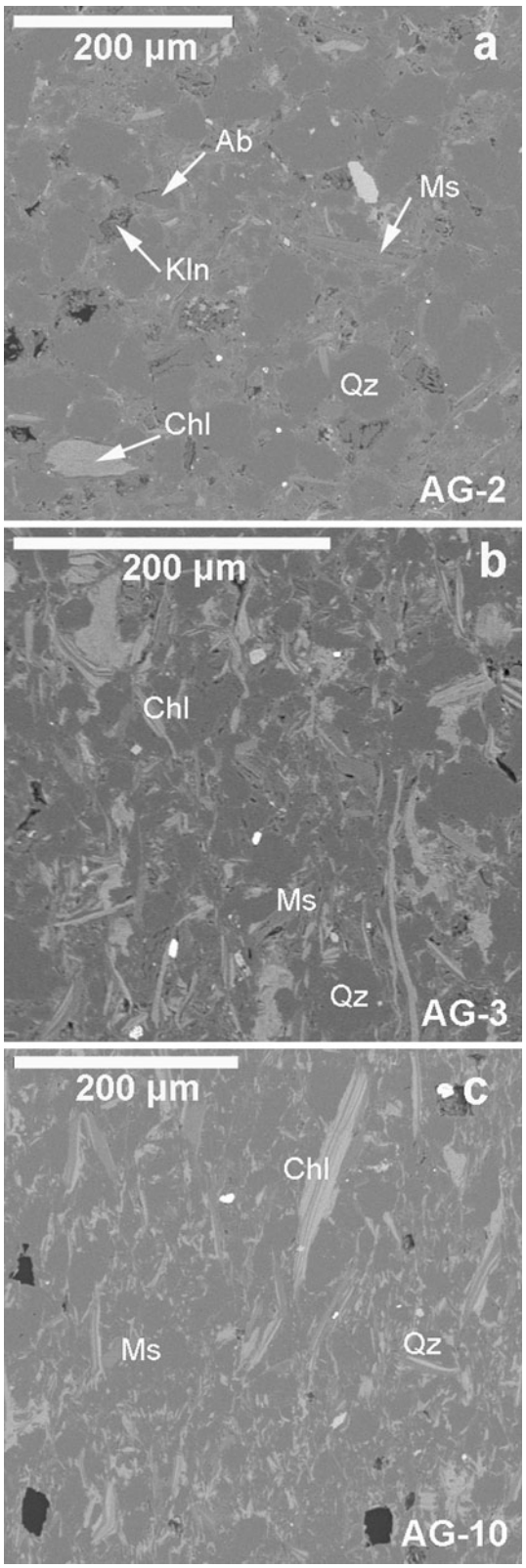

Fig. 8 Backscattered electron (BSE) images showing the fine-grained texture of quartz-rich rocks with microdomains of phyllosilicate minerals. **a** AG-2 sample; **b** AG-3 sample; **c** AG-10 sample. Mineral abbreviations according to Whitney and Evans (2010): *Ab* albite, *Chl* chlorite, *Kln* kaolinite, *Ms* muscovite, *Qz* quartz

plagioclase grains display compositions near to the albite end-member.

5 Discussion

The Arisaig Group provides the most continuous and the best exposure of shallow marine Silurian to Lower Devonian rocks in the Appalachian orogen. This research focuses on mineral and fabrics characterization, crystal-chemical parameters, and chemical composition of the phyllosilicate minerals in the fine-grained rocks. The results pertain to the understanding of the diagenetic/metamorphic evolution of sediments during burial in a basin as well as to the relationship between the orogenic events, deformation, and fabric development in the shallow crust. The Arisaig Group samples are positioned along a composite cross section across shallowly plunging Acadian folds. These folds have variably developed axial planar cleavage, the origin of which is interpreted to be related to transpression linked to dextral movement along the Hollow Fault.

The mineral assemblages in the Arisaig Group samples are, in general, typical of diagenetic to very low-grade metamorphic conditions. Chlorite, muscovite, and quartz are present in all samples. Feldspars (mostly albite) occur in almost all samples, whereas I/S mixed-layers and kaolinite have been identified in the diagenetic samples and Na–K mica in the anchizonal ones. Chlorite-white mica stacks, characteristic of the anchizone were studied by backscattered electron images (Fig. 8c). The chemical composition of dioctahedral micas is quite variable, and shows very low illitic substitution and variable phengitic content. This composition is in agreement with the highly heterogeneous b and d_{001} parameters of the muscovite (Table 1) and with the diagenetic conditions, characterized by the lack of chemical homogenization. The scarcity of paragonitic substitution in the white micas can be related to the presence of albite and the low temperature reached by the samples during the diagenetic and incipient metamorphic stages.

Chemical heterogeneity of phyllosilicates in samples which have not surpassed the deep diagenetic conditions is in part the result of the persistence of detrital phases and their influence on the local composition of the newly formed phases. In these samples, the larger micas preserve their original chemical compositions consistent with their detrital origin and therefore reflect the characteristics of the source area. The inheritance is more significant in samples without deformation fabrics which preserve a sedimentary composition with important presence of silt and sand grain sizes. Therefore, it is not surprising that the micas analysed by SEM (due to analytical limitations those of biggest size) do not show very-low metamorphic compositions, as evidenced by the lack of illitic compositions.

Table 3 Structural formulae for K-rich dioctahedral micas normalized to $O_{10}(OH)_2$ on the basis of scanning electron microscopy (SEM) data

	Si	^{IV}Al	^{VI}Al	Fe	Mg	Mn	Ti	∑oct.	K	Na	∑inter.	Al tot	Fe + Mg
AG2_1_4	3.00	1.00	1.87	0.05	0.04	0.00	0.05	2.02	0.90	0.06	0.96	2.87	0.09
AG2_3A1_1	3.37	0.63	1.64	0.18	0.18	0.00	0.00	2.01	0.80	0.04	0.84	2.27	0.36
AG2_3A2_3	3.24	0.76	1.54	0.21	0.18	0.00	0.07	2.00	0.84	0.07	0.91	2.30	0.40
AG2_3A22_3	3.10	0.90	1.56	0.27	0.11	0.01	0.06	2.01	0.96	0.03	0.99	2.47	0.38
AG2_3A22_2	3.05	0.95	1.34	0.20	0.16	0.00	0.30	2.00	0.79	0.06	0.86	2.29	0.36
AG2_4_10	3.11	0.89	1.72	0.13	0.13	0.00	0.04	2.02	0.90	0.05	0.94	2.61	0.26
AG3_1_1	3.26	0.74	1.46	0.35	0.24	0.00	0.00	2.05	0.92	0.00	0.92	2.19	0.59
AG3_2_2	3.19	0.81	1.71	0.17	0.17	0.00	0.00	2.06	0.73	0.12	0.85	2.52	0.35
AG3_2_3	3.08	0.92	1.62	0.25	0.15	0.00	0.03	2.05	0.89	0.06	0.96	2.54	0.39
AG3_2_10	3.09	0.91	1.83	0.07	0.05	0.00	0.07	2.03	0.57	0.24	0.80	2.74	0.13
AG3_3_3	3.24	0.76	1.39	0.42	0.23	0.00	0.02	2.06	0.88	0.00	0.88	2.15	0.64
AG3_3_5	3.36	0.64	1.45	0.27	0.30	0.00	0.02	2.04	0.88	0.00	0.88	2.09	0.57
AG3_4_4	3.20	0.80	1.53	0.24	0.24	0.00	0.04	2.05	0.91	0.00	0.91	2.33	0.48
AG3_4_7	3.18	0.82	1.70	0.16	0.19	0.00	0.00	2.05	0.86	0.05	0.91	2.52	0.35
AG3_4_10	3.24	0.76	1.51	0.32	0.20	0.00	0.03	2.05	0.84	0.00	0.84	2.27	0.51
AG3_4_12	3.04	0.96	1.91	0.08	0.04	0.00	0.00	2.03	0.65	0.27	0.92	2.87	0.12
AG3_4_13	3.08	0.92	1.70	0.20	0.12	0.00	0.02	2.05	0.83	0.11	0.93	2.62	0.32
AG10_1_5	3.09	0.91	1.57	0.25	0.13	0.00	0.06	2.02	0.97	0.02	0.98	2.47	0.39
AG10_2_1	3.22	0.78	1.56	0.24	0.21	0.00	0.02	2.03	0.86	0.07	0.93	2.33	0.45
AG10_2_2	3.12	0.88	1.72	0.19	0.10	0.00	0.02	2.03	0.87	0.05	0.92	2.60	0.29
AG10_3_4	3.15	0.85	1.52	0.31	0.17	0.00	0.03	2.03	0.89	0.09	0.98	2.36	0.48
AG10_4-3	3.28	0.72	1.58	0.21	0.19	0.00	0.02	2.00	0.87	0.05	0.94	2.30	0.40
AG10_7_3	3.20	0.80	1.56	0.25	0.16	0.00	0.02	2.00	0.97	0.03	1.00	2.37	0.41
AG10_7_4	2.89	1.11	1.57	0.06	0.05	0.00	0.31	1.98	0.84	0.08	0.92	2.67	0.11

Table 4 Structural formulae for chlorites normalized to $O_{10}(OH)_8$ on the basis of scanning electron microscopy (SEM) data

	Si	^{IV}Al	^{VI}Al	Fe	Mg	Mn	Ti	∑oct.	Fe/Fe + Mg	Na	K
AG2_1_5	2.48	1.52	1.46	3.36	1.11	0.07	0.01	6.01	0.75	0.03	0.00
AG2_2_9	3.00	1.00	1.33	2.49	1.95	0.05	0.01	5.83	0.56	0.03	0.02
AG2_3A22_4	2.61	1.39	1.26	3.54	1.22	0.02	0.01	6.05	0.74	0.01	0.01
AG2_4_3	2.85	1.15	1.50	3.46	0.81	0.00	0.03	5.80	0.81	0.02	0.01
AG10_3_1	2.66	1.34	1.56	3.65	0.66	0.01	0.00	5.89	0.85	0.01	0.05
AG3_1_2	2.72	1.28	1.78	3.29	0.67	0.00	0.00	5.75	0.83	0.00	0.00
AG3_1_5	2.75	1.25	1.93	2.96	0.77	0.00	0.00	5.66	0.79	0.00	0.04
AG3_2_7	2.91	1.09	1.73	2.81	1.14	0.00	0.00	5.68	0.71	0.00	0.00
AG3_2_8	2.72	1.28	1.80	3.23	0.71	0.00	0.00	5.74	0.82	0.00	0.00
AG3_2_9	2.86	1.14	1.94	2.99	0.67	0.00	0.00	5.60	0.82	0.00	0.04
AG3_3_1	2.81	1.19	1.87	2.39	1.40	0.00	0.00	5.66	0.63	0.00	0.03
AG3_3_4	2.74	1.26	1.97	3.02	0.65	0.00	0.00	5.65	0.82	0.00	0.00
AG3_4_1	2.85	1.15	1.81	2.93	0.86	0.00	0.03	5.64	0.77	0.00	0.04
AG3_4_5	2.75	1.25	1.87	3.15	0.68	0.00	0.00	5.69	0.82	0.00	0.04
AG3_4_6	2.74	1.26	1.94	3.01	0.71	0.00	0.00	5.66	0.81	0.00	0.06

According to Waldron et al. (1996), the Arisaig Group basin initiated in the Early Llandovery by rapid subsidence in an extensional setting, a scenario which is compatible with the clay-mineral phases identified in these rocks. The oldest Arisaig Group rocks did not reached complete maturation, as evidenced by the lack of correlation between

stratigraphic depth and KI (Fig. 3). Therefore, the diagenetic/metamorphic grade present in the studied rocks probably reflects post-depositional events such as those that occurred either during the Acadian or the Alleghanian orogenic events.

The metamorphic grade of the analyzed samples increases from diagenesis to high anchizone towards the Hollow Fault (with noticeable increases within a ca. 1 km corridor from the surface exposure of the fault, Figs. 2 and 4). Within that corridor, represented by samples AG-6, 7, 9, 10, and 11, KI measured on 10 Å peaks show no difference with the measure on 5 Å peaks and we also found similar values between the air dried and the EG-treated samples. However, outside this 1 km corridor, the KI values (10 Å-air dried, 10 Å-EG and 5 Å-air dried) are significantly different. Mineralogical differences are in agreement with the evolution of metamorphic grade shown by KI, with the presence of higher-grade minerals (such as intermediate Na–K mica), and the absence of those with an inherited origin within the ca. 1 km corridor adjacent to the Hollow Fault.

In relation to the textural features, an incipient cleavage is observed not only in the anchizonal samples (KI <0.42) but also in some of the diagenetic ones (Figs. 7, 8b). Therefore, the slaty cleavage defined by sub-parallel packets of phyllosilicates is not restricted to the anchizonal samples located in the vicinity of the Hollow Fault. Some of the diagenetic samples (with KI ≥0.42 and clearly sedimentary minerals as I/S mixed-layers) show also a significant degree of phyllosilicate orientation. As previously described, these observations suggest that there is no relationship between the KI and the degree of deformation, as expressed by the orientation of phyllosilicates (Fig. 7). In this context, the incipient slaty cleavage defined by subparallel, preferentially oriented, packets of phyllosilicates is found in foliations developed under temperatures corresponding to diagenetic conditions.

The tectonic strain associated with Acadian folding is probably not responsible for the identified prograde changes, which only occur in close vicinity to the Hollow Fault. The axial planar foliation associated with those folds is localized in the central zone of the studied area, i.e. outside the Hollow Fault corridor. Although foliation development produced clear differences of orientation in the phyllosilicates, it did not impart an increase in the metamorphic grade higher than deep diagenesis. Instead, the localization of the prograde changes within 1 km of the Hollow Fault suggests that the migration of fluids along this fault zone may have been the driving mechanism for the increase of the metamorphic grade favouring recrystallization processes and the presence of anchizonal samples close to it (Fig. 4). In addition, the presence in most of the samples of minor quantities of C/S mixed-layers may be the result of a late fluid-mediated event associated to the Hollow Fault. The focused fluid flow is a common feature of major fault zones and has been recently documented in the nearby St. Mary's Basin (Abad et al. 2010).

Although our data provide no independent constraint on the timing of this movement and related fluid flow along the Hollow Fault, several studies suggest that the movement most likely occurred in the Late Carboniferous. A ^{40}Ar–^{39}Ar study of white mica in Arisaig Group rocks yielded ages of ca. 325–320 Ma, even though the sections sampled display no discernable evidence for Carboniferous tectonism (Murphy and Collins 2008). The same study detected white micas of a similar age in coeval strata, also deformed during the Late Devonian Acadian orogeny, that unconformably overlie the Ediacaran-Early Ordovician strata of the Meguma terrane in southern Nova Scotia. These ages are interpreted to reflect distributed fluid flow along major faults in the region, including the Hollow Fault.

Regional syntheses indicate a major change in the evolution of the Canadian Appalachians in the Late Carboniferous which may be a far-field effect of the onset of Laurentia-Gondwana oblique dextral collision (Murphy et al. 2011). This event resulted in reactivation of pre-existing faults, such as the Hollow Fault and created major new faults (e.g. the Chedabucto Fault along the southern boundary of the Antigonish Highlands). The resulting deformation caused clockwise rotation of pre-existing structures as well as regional fluid flow and extensive mineralization (Kontak et al. 2006, 2008). This deformation also resulted in local zones of transtension associated with opening of other nearby basins like the Stellarton Basin, (Yeo and Ruixiang 1987; Waldron 2004), and transpression related deformation (Murphy et al. 2011).

6 Conclusions

The mineral assemblages of the Arisaig Group lithologies are, in general, typical of very low-grade metamorphism. Nevertheless our data identify clear variations in metamorphic grade from anchizone to diagenesis. These variations do not correlate with stratigraphic depth suggesting that grade is not related to the tectonic setting or burial associated with basin development. Similarly, the relatively high-grade samples do not correlate with either foliation development or with the location of fold hinges, implying that variations in KI are not related to either local or regional strains associated with Acadian folding. Instead, our data indicate that prograde metamorphic changes occurred within a corridor adjacent to the Hollow Fault. Fluid circulation associated with movement along this major fault may have been the driving mechanism for

the increasing metamorphism towards it. Regional syntheses indicate that fault motion responsible for prograde metamorphism probably occurred in the Late Carboniferous as a far-field effect of Laurentia–Gondwana collision.

Acknowledgments We are grateful to Sandra Barr, Martine Buatier and Rafael Ferreriro-Mählmann for constructive reviews. Financial support has been supplied by the Research Projects CGL2011-30153-C02-01 (Spanish Ministry of Science and Technology), R1/12/2010/01 (Universidad de Jaén), Research Groups RNM-179 and RNM-325 of the Junta de Andalucía, and Natural Sciences and Engineering Research Council Discovery and Research Capacity grants to JBM. G.G.-A. funding comes from Spanish Education and Science Ministry Project Grant CGL2009-1367 (O.D.R.E. II). G.G.-A. also acknowledges funding from the Mobility Program Grant PR2007-0475 and hospitality at St. Francis Xavier University. Contribution to I.G.C.P. Project 597.

References

Abad, I., Gutiérrez-Alonso, G., Nieto, F., Gertner, I., Becker, A., & Cabero, A. (2003a). The structure and the phyllosilicates (chemistry, crystallinity and texture) of Talas Ala-Tau (Tien-Shan, Kyrgyz Republic): Comparison with more recent subduction complexes. *Tectonophysics, 365*, 103–127.

Abad, I., Murphy, J. B., Nieto, F., & Gutiérrez-Alonso, G. (2010). Diagenesis to metamorphism transition in an epi-sutural basin: The Late Paleozoic St. Mary's basin, Nova Scotia, Canada. *Canadian Journal of Earth Sciences, 47*, 121–135.

Abad, I., Nieto, F., & Gutiérrez-Alonso, G. (2003b). Textural and chemical changes in slate-forming phyllosilicates across the external-internal zones transition in the low-grade metamorphic belt of the NW Iberian Variscan Chain. *Schweizerische Mineralogische und Petrographische Mitteilungen, 83*, 63–80.

Battaglia, S., Leoni, L., & Sartori, F. (2004). The Kübler Index in late diagenetic to low grade metamorphic pelites: A critical comparison of data from 10 A and 5 A peaks. *Clays and Clay Minerals, 52*, 85–105.

Benson, D.G. (1974). *Geology of the Antigonish Highlands, Nova Scotia*. Geological Survey of Canada, Memoir 376.

Bergström, S. H., Huff, W. D., Kolata, D. R., & Melchin, M. J. (1997). Occurrence and significance of Silurian K-bentonite beds at Arisaig, Nova Scotia, eastern Canada. *Canadian Journal of Earth Sciences, 34*, 1630–1643.

Boucot, A. J., Dewey, J. F., Dineley, D. L., Fletcher, R., Fyson, W. K., Griffin, J. G., Hickox, C. F., McKerrow, W. S., & Ziegler, A. M. (1974). *Geology of the Arisaig area, Antigonish County, Nova Scotia*. Boulder: Geological Society of America, Special Paper 139.

Braid, J. A., & Murphy, J. B. (2004). Fold mechanisms in the shallow crust: An example from the Siluro-Devonian Arisaig Group, Antigonish Highlands, Nova Scotia. *Atlantic Geoscience Society Colloquim & Annual General meeting, Moncton, N.B. Abstract with program,* 5.

Braid, J. A., & Murphy, J. B. (2006). Acadian deformation in the shallow crust: An example from the Siluro-Devonian Arisaig Group, Avalon terrane, mainland Nova Scotia. *Canadian Journal of Earth Sciences, 43*, 71–81.

Brown, G. (1961). *The X-ray identification and crystal structures of clay minerals*. London: Mineralogical Society.

Cocks, L. R. M., & Torsvik, T. H. (2002). Earth geography from 500 to 400 million years ago: A faunal and palaeomagnetic review. *Journal of the Geological Society of London, 159*, 631–644.

Dineley, D. L. (1963). Knoydart Formation (Lower Devonian) of Nova Scotia. *Geological Society of America,* Special Paper 73, pp. 138–139.

Escaragga, E., Barr, S. M., Murphy, J. B., & Hamilton, M. A. (2012). Ordovician A-type plutons in the Antigonish Highlands, Nova Scotia. *Canadian Journal of Earth Sciences, 49*, 329–345.

Fortey, R. A., & Cocks, L. R. M. (2003). Palaeontological evidence bearing on global Ordovician-Silurian continental reconstructions. *Earth Science Reviews, 61*, 245–307.

Frey, M. (1987). *Low temperature metamorphism*. Glasgow: Blackie & Sons.

Giorgetti, G., Memmi, I., & Peacor, D. R. (2000). Retarded illite crystallinity caused by stress-induced sub-grain boundaries in illite. *Clay Minerals, 35*, 693–708.

Guidotti, C. V., Mazzoli, C., Sassi, F. P., & Blencoe, J. G. (1992). Compositional controls on the cell dimensions of $2M_1$ muscovite and paragonite. *European Journal of Mineralogy, 4*, 283–297.

Guidotti, C. V., Yates, M. G., Dyar, M. D., & Taylor, M. E. (1994). Petrogenetic implications of the Fe^{3+} content of muscovite in pelitic schists. *American Mineralogist, 79*, 793–795.

Gutiérrez-Alonso, G., Fernández-Suárez, J., Weil, A. B., Murphy, J. B., Nance, R. D., Corfú, F., et al. (2008). Self-subduction of the Pangean global plate. *Nature Geoscience, 1*, 549–553.

Gutiérrez-Alonso, G., & Nieto, F. (1996). White-mica "cristallinity", finite strain and cleavage development across a large Variscan structure, NW Spain. *Journal of the Geological Society, London, 153*, 287–299.

Hamilton, M. A., & Murphy, J. B. (2004). Tectonic significance of a Llanvirn age for the Dunn Point volcanic rocks, Avalon terrane, Nova Scotia, Canada: Implications for the evolution of the Iapetus and Rheic oceans. *Tectonophysics, 379*, 199–209.

Hurst, J. M., & Pickerill, R. K. (1986). The relationship between sedimentary facies and faunal associations in the Llandovery siliciclastics Ross Brook Formation, Arisaig, Antigonish County, Nova Scotia. *Canadian Journal of Earth Sciences, 23*, 711–716.

Keppie, J. D. (1985). The Appalachian Collage. In D. G. Gee & B. Sturt (Eds.), *The Caledonide Orogen, Scandinavia, and related areas* (pp. 1217–1226). New York: Wiley.

Kisch, H. J. (1991). Illite crystallinity: Recommendations on sample preparation, X-ray diffraction settings, and interlaboratory samples. *Journal of Metamorphic Geology, 9*, 665–670.

Kontak, D. J., Archibald, D. A., Creaser, R. A., & Heaman, L. M. (2008). Dating hydrothermal alteration and IOCG mineralization along a terrane-bounding fault zone: The Copper Lake deposit, Nova Scotia. *Atlantic Geology, 44*, 146–166.

Kontak, D. J., Kyser, K., Gize, A., & Marshall, D. (2006). Structurally controlled vein barite mineralization in the Maritimes Basin of eastern Canada: Geologic setting, stable isotopes and fluid inclusions. *Economic Geology, 101*, 407–430.

Kübler, B. (1968). Evaluation quantitative du métamorphisme par la cristallinité de l'illite. *Bulletin du Centre de Recherches Pau-SNPA, 2*, 385–397.

Landing, E. (2005). Early Paleozoic Avalon-Gondwana unity: An obituary-response to **"**Palaeontological evidence bearing on global Ordovician-Silurian continental reconstructions" by R.A. Fortey & L.R.M. Cocks. *Earth-Science Reviews, 69*, 169–175.

Landing, E., & Murphy, J. B. (1991). Uppermost Precambrian (?)—Lower Cambrian of mainland Nova Scotia: Faunas, depositional environments and stratigraphic revision. *Journal of Paleontology, 65*, 382–396.

Lane, T. E., & Jensen, L. R. (1975). Stratigraphy of the Arisaig Group. *Maritime Sediments, 11*, 119–140.

Merriman, R. J., & Peacor, D. R. (1999). Very low-grade metapelites: Mineralogy, microfabrics and measuring reaction progress. In M. Frey & D. Robinson (Eds.), *Low grade-metamorphism* (pp. 10–60). Oxford: Blackwell Science.

Meyer, E. M., Burgreen, B. N., Lackey, H., Landis, J. D., Quicksall, A. N., & Bostick, B. C. (2008). Evidence for basin restriction during syn-collisional basin formation in the Silurian Arisaig Group, Nova Scotia. *Chemical Geology, 256*, 1–11.

Murphy, J. B. (1987). The stratigraphy and depositional environment of upper Ordovician to lower Devonian rocks in the Antigonish Highlands, Nova Scotia. *Maritime Sediments and Atlantic Geology, 23*, 63–75.

Murphy, J. B., & Collins, A. J. (2008). Alleghanian overprint on Siluro-Devonian siliciclastic sequences in the Meguma and Avalon terranes in mainland Nova Scotia: Implications for Late Paleozoic tectonic activity. *Tectonophysics, 461*, 265–276.

Murphy, J. B., Fernández-Suárez, J., Jeffries, T. E., & Strachan, R. A. (2004). LA-ICP-MS U-Pb detrital zircon data from Cambrian clastic rocks in Avalonia: Erosion of a Neoproterozoic arc along the northern Gondwanan margin. *Journal of the Geological Society of London, 161*, 243–254.

Murphy, J. B., Gutierrez-Alonso, G., Nance, R. D., Fernandez-Suarez, J., Keppie, J. D., Quesada, C., et al. (2006). Origin of the Rheic Ocean: Rifting along a Neoproterozoic suture? *Geol, 34*, 325–328.

Murphy, J. B., & Keppie, J. D. (1998). Late Devonian palinspastic reconstruction of the Avalon-Meguma terrane boundary: Implications for terrane accretion and basin development in the Appalachian orogen. *Tectonophysics, 284*, 221–231.

Murphy, J. B., Keppie, J. D., Dostal, J., Waldron, J. W. F., & Cude, M. P. (1996). Geochemical and isotopic characteristics of Early Silurian clastic sequences in Antigonish Highlands, Nova Scotia, Canada: Constraints on the accretion of Avalonia in the Appalachian- Caledonide Orogen. *Canadian Journal of Earth Sciences, 33*, 379–388.

Murphy, J. B., Keppie, J. D., & Hynes, A. J. (1991). *Geology of the Antigonish Highlands*. Geological Survey of Canada, Paper 89-10.

Murphy, J. B., & Nance, R. D. (2002). Nd-Sm isotopic systematics as tectonic tracers: An example from West Avalonia, Canadian Appalachians. *Earth Science Reviews, 59*, 77–100.

Murphy, J. B., Nance, R. D., & Keppie, J. D. (1999). Fault reactivation within Avalonia: Plate margin to continental interior deformation. *Tectonophysics, 305*, 183–204.

Murphy, J. B., Waldron, J. W. F., Kontak, D. J., Pe-Piper, G., & Piper, D. J. W. (2011). Minas Fault Zone: Late Paleozoic history of an intra-continental orogenic transform fault in the Canadian Appalachians. *Journal of Structural Geology, 33*, 312–328.

Nance, R. D., Gutiéerrez-Alonso, G., Keppie, J. D., Linnemann, U., Murphy, J. B., Quesada, C., et al. (2010). Evolution of the Rheic Ocean. *Gondwana Research, 17*, 194–222.

Nance, R. D., & Murphy, J. B. (1994). Contrasting basement isotopic signatures and the palinspastic restoration of peripheral orogens; example from the Neoproterozoic Avalonian-Cadomian Belt. *Geol, 22*, 617–620.

Nieto, F., Ortega-Huertas, M., Peacor, D. R., & Aróstegui, J. (1996). Evolution of illite/smectite from early diagenesis through incipient metamorphism in sediments of the Basque-Cantabrian Basin. *Clays and Clay Minerals, 44*, 304–323.

Nieto, F., & Sanchez-Navas, A. (1994). A comparative XRD and TEM study of the physical meaning of the white mica "crystallinity" index. *European Journal of Mineralogy, 6*, 611–621.

Pickerill, R. K., & Hurst, J. M. (1983). Sedimentary facies, depositional environments, and faunal associations of the lower Llandovery (Silurian) Beechill Cove Formation. *Canadian Journal of Earth Sciences, 20*, 1761–1779.

Reinhardt, J. (1991). Low-pressure, high-temperature metamorphism in a compressional tectonic setting (Mary Kathleen Fold Belt, NE Australia). *Geological Magazine, 129*, 41–57.

Rodríguez-Navarro, A. B. (2006). XRD2Dscan: New software for polycrystalline material characterization using two-dimensional X-ray diffraction. *Journal of Applied Crystallography, 39*, 905–909.

Sassi, F. P., & Scolari, A. (1974). The b_0 value of the potassic white micas as a barometric indicator in low-grade metamorphism of pelitic schists. *Contributions to Mineralogy and Petrology, 45*, 143–152.

Strachan, R. A., & Taylor, G. K. (Eds.). (1990). *Avalonian and Cadomian rocks of the North Atlantic*. Glasgow: Blackie & Sons.

Theokritoff, G. (1979). Early Cambrian provincialism and biogeographic boundaries in the North Atlantic region. *Lethaia, 12*, 281–295.

van Staal, C. R., Dewey, J. F., Mac Niocaill, C., & McKerrow, W. S., (1998). The Cambrian-Silurian tectonic evolution of the Northern Appalachians and British Caledonides: History of a complex, west and southwest Pacific-type segment of Iapetus. In D. Blundell & A. C. Scott (Eds.), *Lyell: The past is the key to the present* (pp. 199–242). Geological Society of London Special Publication 143.

van Staal, C. R., Whalen, J. B., Valverde-Vaquero, P., Zagorevski, A., & Rogers, N. (2009). Pre-Carboniferous, episodic accretion-related, orogenesis along the Laurentian margin of the northern Appalachians. In J. B. Murphy, J. D. Keppie & A. J. Hynes, (Eds.), *Ancient Orogens and Modern Analogues* (pp. 271–316). Geological Society of London Special Publication 327.

Waldron, J. W. F. (2004). Anatomy and evolution of a pull-apart basin, Stellarton, Nova Scotia. *Geological Society of America Bulletin, 116*, 109–127.

Waldron, J. W. F., Murphy, J. B., Melchin, M., & Davis, G. (1996). Silurian tectonics of western Avalonia: Strain corrected subsidence history of the Arisaig Group, Nova Scotia. *Journal of Geology, 104*, 677–694.

Warr, L. N., & Rice, H. N. (1994). Interlaboratory standardization and calibration of clay mineral crystallinity and crystallite size data. *Journal of Metamorphic Geology, 12*, 141–152.

Whitney, D. L., & Evans, B. W. (2010). Abbreviations for names of rock-forming minerals. *American Mineralogist, 95*, 185–187.

Woodcock, N. H., Soper, N. J., & Strachan, R. A. (2007). A Rheic cause for the Acadian deformation in Europe. *Journal of the Geological Society, 164*, 1023–1036.

Yeo, G. M., & Ruixiang, G. (1987). Stellarton Graben: An Upper Carboniferous pull-apart basin in Nova Scotia. In C. Beaumont & A. J. Tankard, (Eds.), *Sedimentary basins and basin-forming mechanisms* (pp. 299–309). Canadian Society of Petroleum Geologists Memoir 12.